Electronic Supplementary Material (ESI)

Structure and Stability of 7-mercapto-4-methylcoumarin Self-Assembled Monolayers on Gold: an Experimental and Computational analysis.

Davide Marchi[1], Eleonora Cara[2], Federico Ferrarese Lupi[2], Philipp Hönicke[3], Yves Kayser[3], Burkhard Beckhoff[3], Micaela Castellino[4], Petr Klapetek[5], Alberto Zoccante[1], Michele Laus[1], and Maurizio Cossi[1]

1) Dipartimento di Scienze e Innovazione Tecnologica (DISIT), Università del Piemonte Orientale, via T. Michel 11, I-15121, Alessandria, Italy
2) Istituto Nazionale di Ricerca Metrologica (INRIM), Strada delle Cacce, 91, I-10135, Torino, Italy
3) Physikalisch-Technische Bundesanstalt (PTB), Abbestr. 2-12, 10587 Berlin, Germany.
4)Department of Applied Science and Technology, Politecnico di Torino, C.so Duca degli Abruzzi 24, 10129 Turin, Italy.
5) Department of Nanometrology, Czech Metrology Institute, Okružní 31, 638 00 Brno, Czech Republic

1) Parameterization of the Force Field (FF).

The FF parameters for MMC were taken from GROMOS 54A7 set as provided by the Automated Topology Builder (ATB) website.
The FF was used without changes to model bonded interactions as well as the repulsion-dispersion interactions between the organic molecules. The FF reliability to reproduce the intermolecular interactions was checked by performing a rigid scan of a MMC dimer, comparing the classical intermolecular energies computed with LAMMPS program and GROMOS 54A7 force field, and the QM energies obtained with DFT (see below for the level of calculation). The very good agreement, shown in Figure S1, indicates that MMC/MCM interactions are fairly reproduced with this FF.

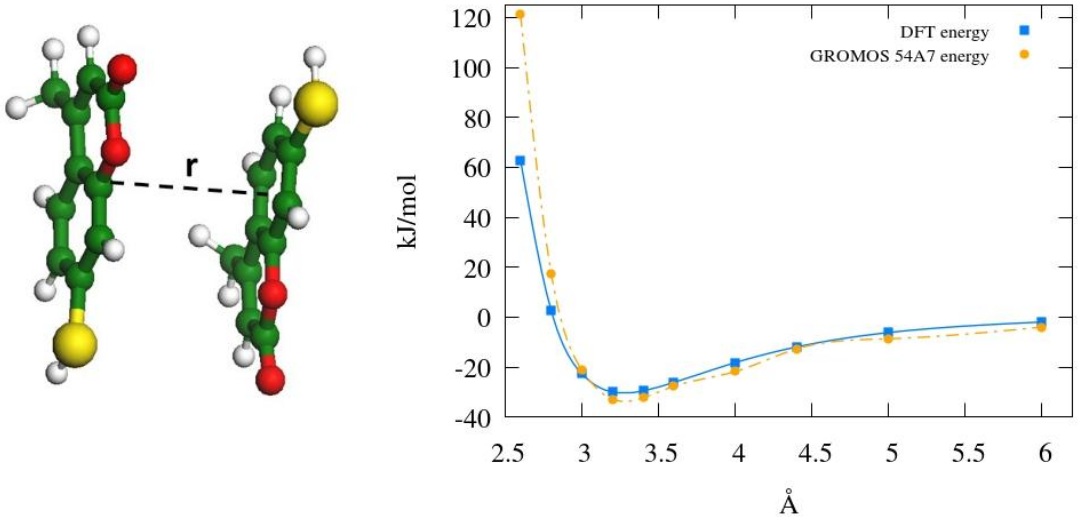

Figure S1. Comparison of MMC dimer intermolecular energies (kJ/mol) along a rigid scan of the intermolecular distance *r*, computed with DFT and GROMOS FF.

On the other hand, the interactions of MMC molecules and radicals with the gold surface were described with pairwise non-bonding parameters fitted in this work on DFT calculations as detailed below.

We decided to model with 6-12 Lennard-Jones (LJ) function both –SH · · ·Au and –S · · ·Au interactions, though the latter can be considered a real covalent bond, to allow thiyl units to shift on the surface and possibly also leave too crowded monolayers. Note that the GROMOS 54A7 FF used to compute MMC/MMC interactions includes a Coulomb contribution through point charges obtained by fitting DFT electrostatic potentials; for MMC/gold interactions, instead, we did not include Coulomb terms, fitting the whole interaction energy with LJ terms only.

A gold cluster of 60 atoms (5x4x3) was cleaved from a periodic three-layers thick (111) slab, previously optimized in CRYSTAL17 at the DFT/PW91 level with the basis set and pseudopotentials for core electrons of Hay and Wadt [1].

The molecule set used for the fitting procedure is reported in Table S1, along with the atom types and symbols used in the force field. In order to obtain a set of LJ parameters with minimal correlation, the fit was carried out incrementally, determining the optimal FF parameters for one or two atom types at each step.

Molecule	**Atom types fitted**	**Atom types symbol**
Benzene	Aromatic C, H	CA, HA
Benzenethiol	Thiol S, H	SH, HB
Methylbenzenethiol	sp^3 C, aliphatic H	C3, H
7-mercapto-4-methylcoumarin (MMC)	Oxygen	O
MMC thiyl radical	Thiyl S	S

Table S1. Molecule set used for the fitting procedure; the atom types and symbols fitted at each step are reported as well.

A geometry optimization was performed at the DFT/B3LYP level, using the Gaussian16 suite, for each molecule in Table S1 in close proximity with the surface of the gold cluster. Then, the distance between the molecule and the gold slab was varied incrementally, while keeping the molecular geometry fixed. At each step, the DFT energy of interaction between the molecule and the slab was computed. The basis set and pseudopotentials of Hay and Wadt [1] were used for gold atoms, while Dunning's correlation consistent cc-pVDZ [2] basis set was used for all other elements. Grimme's dispersion energy correction [3] was included in all calculations, and the basis set superposition error (BSSE) was corrected through the counterpoise method, as implemented in Gaussian16.

For benzene and benzenethiol, additional scans were performed keeping the plane of the aromatic ring perpendicular to the gold surface. This geometry is meant to mimic the preferred orientation in densely packed SAMs, a target system that the force field should describe correctly.

Finally, we optimized additional LJ parameters to describe the S-Au interactions involving MMC thiyl radicals. Though thiyls are expected to form covalent bonds with gold atoms, we used LJ functional form for this pair also, instead of the most used harmonic potential for instance, because

to equilibrate the monolayers the thiyl units must be able to glide laterally on the metal surface, or even leave the surface if this lowers the energy of the system.
The fitting procedure was carried out on the model systems and configurations described above through an ad hoc python script. The script was interfaced with LAMMPS program to obtain single-point molecular mechanics energies, then the force field parameters were iteratively varied by employing the trust region reflective algorithm, up to fitting DFT energies.
All the optimized parameters are listed in Table S2; the complete FF in the GROMACS format (itp files) is also provided in the ESI.

Pair	ε (kcal/mol)	σ (Å)
Au – CA	0.571	3.228
Au – C3	0.775	2.996
Au – HA	0.020	2.975
Au – HB	0.500	2.555
Au – H	0.100	3.114
Au – O	0.146	3.435
Au – SH	1.169	3.243
A – S	13.406	2.230

Table S2. Lennard-Jones parameters for Au-X pair interactions in the FF fitted to DFT calculations.

The reliability of the fitting procedure can be appreciated by the good agreement between DFT and FF energies with the fitted parameters for the whole set of molecules, illustrated in Figure S2.

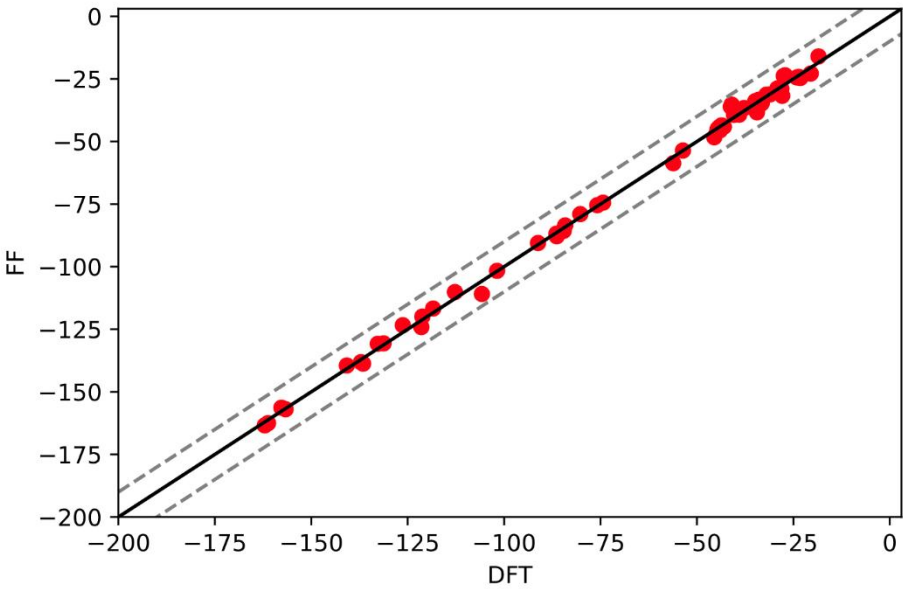

Figure S2. Comparison between the fitted FF and DFT energies (kJ/mol) for the whole set of molecules used in the fitting procedure. The black solid line denotes 1:1 correlation, while the gray dotted lines represent ±10 kJ/mol marks.

To evaluate the performance of the FF in working conditions, however, one has to explore the conformational space of MMC on Au surface more widely, considering other orientations beside the scan used in the fitting, and allowing geometry deformations.
To do that, we performed a MD at 298 K (1 ns equilibration, 2 ns production) for a set of 253 MMC thiol molecules on the gold periodic surface described in the manuscript: the number of molecules was chosen to allow the formation of a second layer also (see main text), improving the sampling of MMC/Au distances. Thirty equally spaced snapshots were extracted from the production MD run, and from each snapshot a nonperiodic cluster was cut, including 60 (5x4x3) Au atoms and one MMC molecule selected randomly. The MMC/surface interaction energy was then computed for each cluster with the optimized FF and with DFT. The comparison is shown in Figure S3: two distinct sets of energies are clearly visible, corresponding to molecules either in the SAM or in the second layer. The agreement is satisfactory, even if the classical energies tend to be somehow overestimated for strongly bound molecules: however, the errors with respect to ab initio energies are limited to 5-10% for almost all the considered conformations, ensuring the reliability of the model.

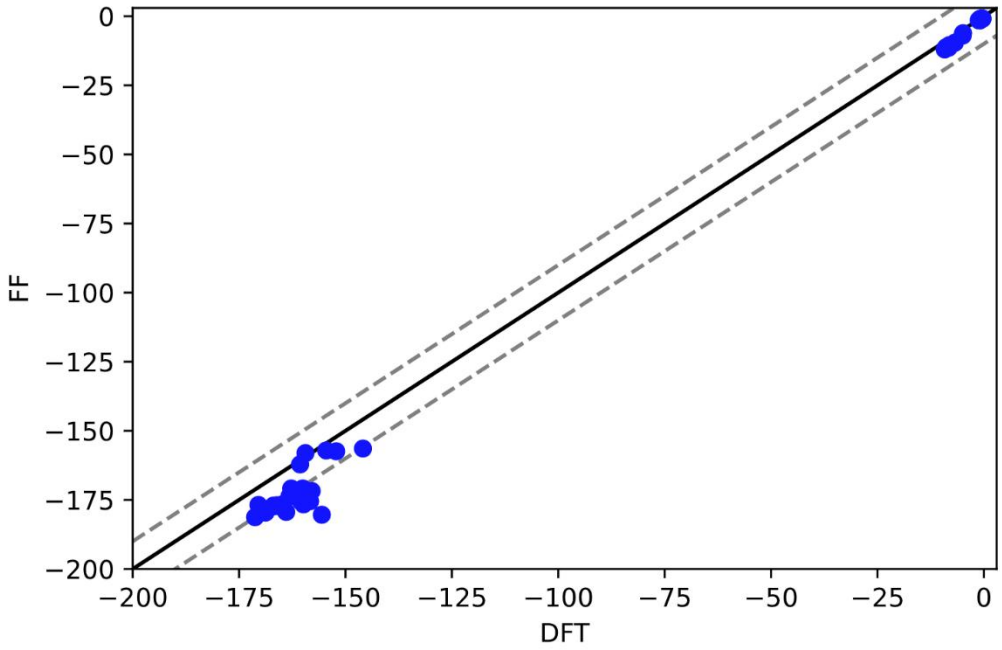

Figure S3. Comparison between the fitted FF and DFT energies (kJ/mol) for thirty clusters including 60 Au atoms and one MMC thiol molecule in random position and orientation. The black solid line denotes 1:1 correlation, while the gray dotted lines represent ±10 kJ/mol marks.

2) Free energy evaluation through BAR method.

In the Bennet Acceptance Ratio (BAR) method a coupling parameter λ (varying from 1 to 0 as the system shifts from real to decoupled) is defined to gradually switch off the intermolecular interactions between the target molecule and the rest of the system: first, Coulomb interactions are removed in 20 steps while vdW interactions remain unaltered, then also vdW terms are eliminated in 20 further steps, until the target unit is completely decoupled. For each λ value, a MD run is performed comprising 0.5 ns equilibration (timestep 0.5 fs) and 1 ns production (timestep 1 fs).

3) Measurement of the metallic surface area.

The gold surface of a non-functionalized sample was scanned by atomic force microscopy (AFM) to determine the factor *k* (manuscript equation 1), i.e. the ratio between the surface area and the projected area. The AFM used (Bruker Dimension Icon) was calibrated using a step height standard against an interferometric AFM. The measurements were conducted with two tips for hard tapping mode (Bruker RTESPA-525) in order to account for the tip wear and convolution. Several scans of the gold surface were carried out on large areas (25 μm^2, 2048x2048 pixels, Figure S4) compared to the autocorrelation length of the roughness (~10 nm) in order to prevent leveling to affect the statistical results [1]. The factor *k* was evaluated through the statistical analysis tool in Gwyddion open source software [2] finding a value of (1.0076 ± 0.0014). Consequently, the 1/*k* correction factor in manuscript equation (1) was evaluated as (0.9925 ± 0.0014). For the uncertainty computation, additional measurements were performed in non-ideal conditions and simulations were performed using synthetic tools in Gwyddion [3], considering the variations across the sample, giving the largest contribution, microscope calibration, leveling, feedback loop faults, noise and tip convolution. The microscope noise was found to be most critical experimental parameter, related to the small sample roughness (roughness parameter S_q = 0.9 nm) and measurements had to be carefully optimized for achieving low noise floor (~30 pm).

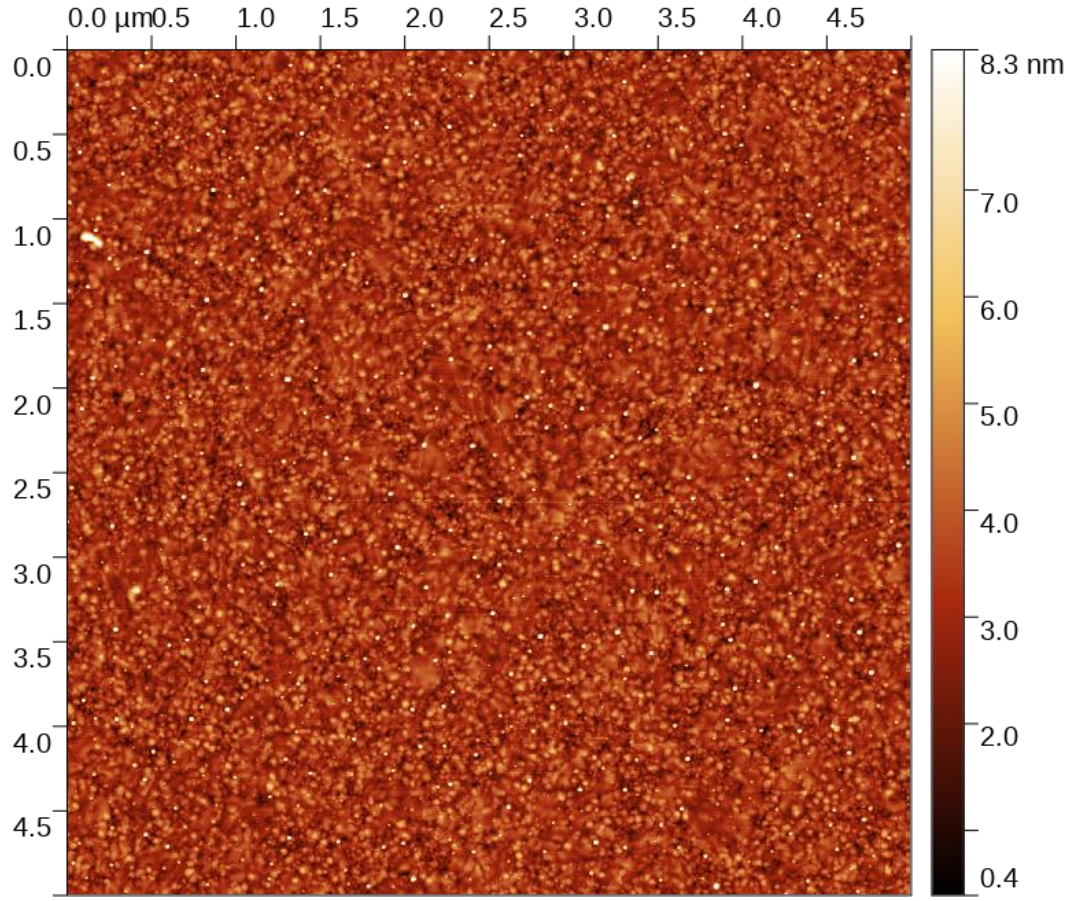

Figure S4. AFM scanning map of the gold area used to determine the 1/*k* correction factor in manuscript equation (1).

4) Details of GIXRF characterization.

GIXRF experiment was conducted at the four crystal monochromator (FCM) beamline for bending magnet radiation [4] at BESSY II synchrotron radiation facility.The reference-free GIXRF experiments were performed employing in-house built instrumentation [5], which allows for precise sample alignment and angular variations of the sample with respect to the incident photon beam.

The optimization of the excitation conditions for sulfur K-shell X-ray fluorescence was obtained by minimizing the contributions of Au M-shell X-ray fluorescence to the experimental spectra. To this goal, an incident photon energy of E_0 = 2.6 keV was chosen. During the GIXRF scans, the angle of incidence (defined between sample surface and incident X-ray beam) was varied between 0° and 7° with varying stepsize. At each angular position, a fluorescence spectrum was recorded by means of a calibrated [6] silicon drift detector (SDD) mounted at 90° with respect to the incident beam. Additional calibrated photodiodes on a separate 2θ axis allow for both X-ray reflectometry (XRR) measurements for the determination of the X-ray standing wave (XSW) as well as for a determination of the incident photon flux Φ_0. To separate the sulfur signal from the recorded spectra, a spectral deconvolution procedure was implemented employing detector response functions [6] for relevant X-ray fluorescence lines as well as physical models for the relevant background contributions, e.g. bremsstrahlung from the sample matrix. In the case of sulfur on gold, this deconvolution procedure is essential as there is a relatively strong overlap of sulfur Ka radiation and the gold M5 and M4 lines (Figure 3b). For this reason, the latter has been deconvoluted employing fixed line sets for all the gold M5 lines as a single object (and the same for gold M4) as already discussed in reference 7.

5) Details of XPS characterization.

The semi-quantitative atomic concentration and fitting procedures were acquired using CasaXPS 2.3.23 dedicated software (Casa Software Ltd.,Wilmslow, UK). All core-level peak energies were referenced to C1s peak at 284.5 eV and the background contribution in HR scans was subtracted by means of a Shirley function.

A spot size of 100 μm was used to collect the photoelectron signal for both the high resolution (HR) and the survey spectra.

Different pass energy values were employed: 187.8 eV for survey spectra and 23.5 eV for HR peaks. Survey scans (from 1200 to 0 eV, energy step ΔE = 1 eV) have been performed as the first step measurements to detect all the elements on sample surfaces.

HR scans have been performed only in smaller ranges in the Binding Energy (BE) scale (energy step ΔE = 0.1 eV) around chemical element peaks of major interest for this study, i.e. C(1s), O(1s), S(2p) and Au(4f).

6) High density thiyl SAM.

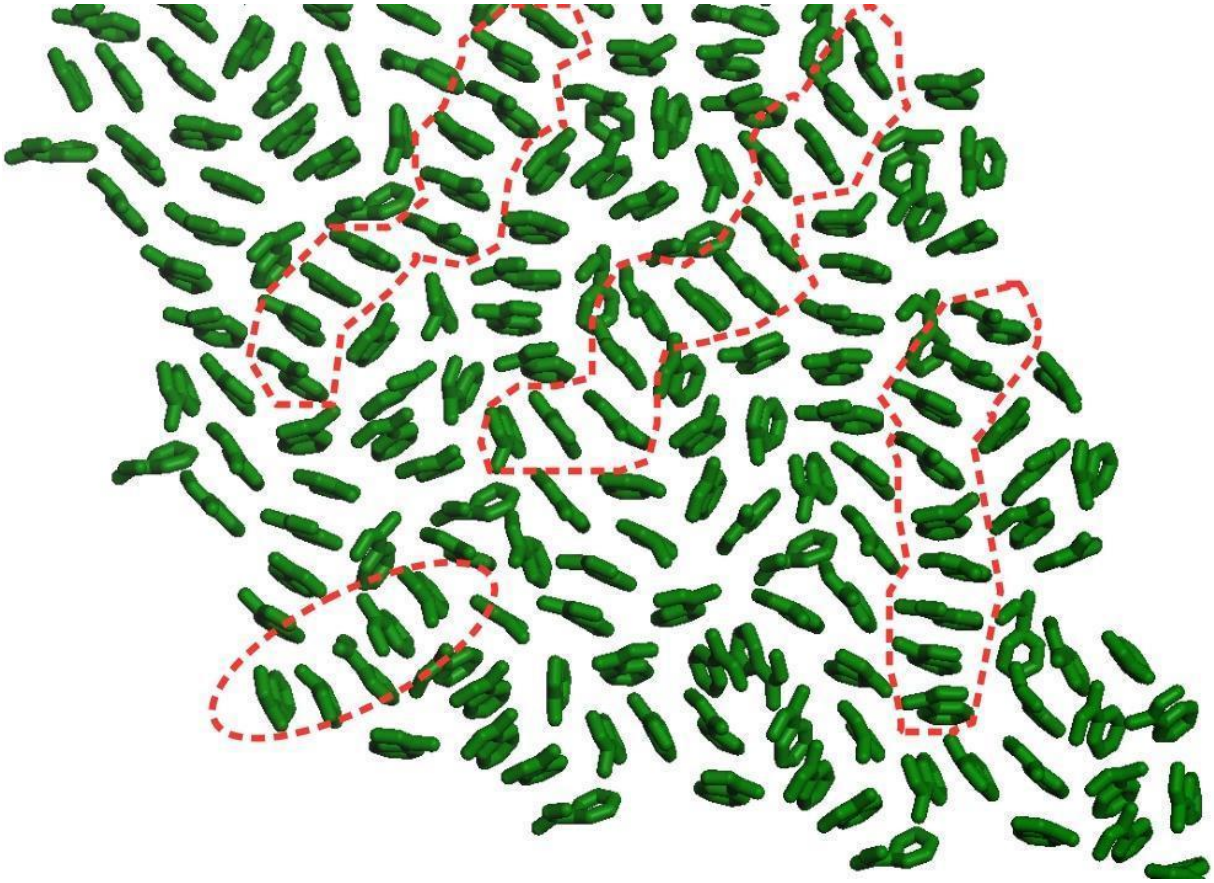

Figure S5. Some ordered stackings of MMC thiyl units in the densest monolayer (4.8 nm^{-2})

References

[1] Nečas, D.; Valtr, M.; Klapetek, P. How levelling and scan line corrections ruin roughness measurement and how to prevent it. Scientific reports 2020, 10 (1), 1-15.

[2] Nečas, D.; Klapetek, P. Gwyddion: an open-source software for SPM data analysis. Open Physics 2012, 10 (1), 181-188.

[3] Nečas, D.; Klapetek, P. Synthetic Data in Quantitative Scanning Probe Microscopy. Nanomaterials 2021, 11 (7), 1746.

[4] Krumrey, M.; Ulm, G. *Nuclear Instruments and Methods in Physics Research Section A: Accelerators, Spectrometers, Detectors and Associated Equipment*, 2001, 467, 1175–1178.

[5] Lubeck, J.; Beckhoff, B.; Fliegauf, R.; Holfelder, I.; Hönicke, P.; Müller, M.; Pollakowski, B.; Reinhardt, F.; Weser, J. *Review of Scientific Instruments*, 2013, 84, 045106.

[6] Scholze, F.; Procop, M. *X-Ray Spectrometry: An International Journal* 2009, 38, 312–321.

[7] Kolbe, M.; Hönicke, P.; Müller, M.; Beckhoff, B. *Physical Review A*, 2012, 86, 042512